Comparison of HepaRG and HepG2 cell lines to model mitochondrial respiratory adaptations in non-alcoholic fatty liver disease

TUMISANG EDWARD MASEKO[1], MOUSTAFA ELKALAF[1], EVA PETEROVÁ[1,2], HALKA LOTKOVÁ[1], PAVLA STAŇKOVÁ[1], JAN MELEK[1], JAN DUŠEK[1,3], PETRA ŽÁDNÍKOVÁ[1], DANA ČÍŽKOVÁ[4], ALEŠ BEZROUK[5], PETR PÁVEK[3], ZUZANA ČERVINKOVÁ[1] and OTTO KUČERA[1]

Departments of [1]Physiology and [2]Medical Biochemistry, Charles University, Faculty of Medicine in Hradec Kralove, 500 03 Hradec Kralove; [3]Department of Pharmacology and Toxicology, Charles University, Faculty of Pharmacy in Hradec Kralove, 500 05 Hradec Kralove; Departments of [4]Histology and Embryology, and [5]Medical Biophysics, Charles University, Faculty of Medicine in Hradec Kralove, 500 03 Hradec Kralove, Czech Republic

Received June 26, 2023; Accepted December 1, 2023

DOI: 10.3892/ijmm.2023.5342

Abstract. Although some clinical studies have reported increased mitochondrial respiration in patients with fatty liver and early non-alcoholic steatohepatitis (NASH), there is a lack of *in vitro* models of non-alcoholic fatty liver disease (NAFLD) with similar findings. Despite being the most commonly used immortalized cell line for *in vitro* models of NAFLD, HepG2 cells exposed to free fatty acids (FFAs) exhibit a decreased mitochondrial respiration. On the other hand, the use of HepaRG cells to study mitochondrial respiratory changes following exposure to FFAs has not yet been fully explored. Therefore, the present study aimed to assess cellular energy metabolism, particularly mitochondrial respiration, and lipotoxicity in FFA-treated HepaRG and HepG2 cells. HepaRG and HepG2 cells were exposed to FFAs, followed by comparative analyses that examained cellular metabolism, mitochondrial respiratory enzyme activities, mitochondrial morphology, lipotoxicity, the mRNA expression of selected genes and triacylglycerol (TAG) accumulation. FFAs stimulated mitochondrial respiration and glycolysis in HepaRG cells, but not in HepG2 cells. Stimulated complex I, II-driven respiration and β-oxidation were linked to increased complex I and II activities in FFA-treated HepaRG cells, but not in FFA-treated HepG2 cells. Exposure to FFAs disrupted mitochondrial morphology in both HepaRG and HepG2 cells. Lipotoxicity was induced to a greater extent in FFA-treated HepaRG cells than in FFA-treated HepG2 cells. TAG accumulation was less prominent in HepaRG cells than in HepG2 cells. On the whole, the present study demonstrates that stimulated mitochondrial respiration is associated with lipotoxicity in FFA-treated HepaRG cells, but not in FFA-treated HepG2 cells. These findings suggest that HepaRG cells are more suitable for assessing mitochondrial respiratory adaptations in the developed *in vitro* model of early-stage NASH.

Correspondence to: Dr Otto Kučera, Department of Physiology, Charles University, Faculty of Medicine in Hradec Kralove, Simkova 870, 500 03 Hradec Kralove, Czech Republic
E-mail: kucerao@lfhk.cuni.cz

Abbreviations: BSA, bovine serum albumin; CPT1A, carnitine palmitoyltransferase 1A; CS, citrate synthase; DGAT2, diacylglycerol O-acyltransferase 2; ECAR, extracellular acidification rate; FASN, fatty acid synthase; FCCP, carbonyl cyanide-4-(trifluoromethoxy) phenylhydrazone; FFA, free fatty acid; HADHA, hydroxy acyl-CoA dehydrogenase trifunctional multienzyme complex subunit alpha; LCAD, acyl-CoA dehydrogenase; LDH, lactate dehydrogenase; MMP, mitochondrial membrane potential; MRC, maximal respiratory capacity; NADH, nicotinamide adenine dinucleotide; NAFLD, non-alcoholic fatty liver disease; NASH, non-alcoholic steatohepatitis; OA, sodium oleate; OCR, oxygen consumption rate; OXPHOS, oxidative phosphorylation; PA, sodium palmitate; PC, palmitoyl-carnitine; PPARA, peroxisome proliferator-activated receptor alpha gene; PPARGC1A, peroxisome proliferator-activated receptor gamma coactivator 1-alpha; PRH, primary rat hepatocytes; ROS, reactive oxygen species; TAG, triacylglycerol; TEM, transmission electron microscopy

Key words: non-alcoholic fatty liver disease, steatosis, lipotoxicity, HepaRG cells, HepG2 cells, *in vitro* models, mitochondria, mitochondrial respiration

Introduction

The incidence of non-alcoholic fatty liver disease (NAFLD) continues to increase, mainly due to the increased prevalence of metabolic syndrome, thus rendering NAFLD the most common chronic liver disorder globally (1). It may affect 70-90% of the diabetic population and up to 70% of obese individuals (1). It has also been reported to affect up to 37% of obese children (2). NAFLD includes a spectrum of histological findings ranging from simple steatosis to non-alcoholic steatohepatitis (NASH), liver cirrhosis and hepatocellular carcinoma (3). Of note, ~37% of adult patients with simple steatosis will develop NASH, which is strongly associated with

more detrimental outcomes (4). Although there are contradictory findings regarding the role of mitochondrial dysfunction in the pathogenesis and progression of NAFLD, a substantial body of evidence supports impaired mitochondrial adaptation as a crucial component (5,6). Hepatic oxidative functions are essential in maintaining energy and cellular homeostasis through multiple pathways: β-oxidation, the tricarboxylic acid (TCA) cycle, respiratory chain activity, ketogenesis, glycolysis and ATP synthesis (7,8). Disruptions in these pathways may lead to an impaired energy homeostasis, resulting in aberrant liver functions (5). Although some clinical studies have reported increased mitochondrial respiration in patients with simple steatosis and early-stage NASH (9,10), there is a lack of *in vitro* models of NAFLD demonstrating similar findings (11-13).

Despite the increasing trend to publish 3D or 2D coculture *in vitro* models of NAFLD, the systematic review by Ramos *et al* (13) demonstrated that up to 60% of researchers still predominantly favor 2D monocultures. The use of primary human hepatocytes is ethically and economically limited; thus, primary rodent hepatocytes and immortalized cell lines are attractive for developing 2D *in vitro* models for NAFLD, evaluating cellular metabolism and assessing potential therapeutic compounds (14). HepG2 cells have been the most common immortalized cell line used for 2D *in vitro* models of NAFLD (12). However, studies have demonstrated that decreased mitochondrial respiration observed in free fatty acid (FFA)-treated HepG2 cells was not optimally associated with findings from patients diagnosed with simple steatosis or early-stage NASH, but instead was associated more with late stages of NASH (15-17). In addition, studies have also shown that HepG2 cells have a decreased ability to secrete very low-density lipoproteins, and they exert a low expression of some nuclear receptors, affecting lipid metabolism (18,19). On the other hand, HepaRG cells have exhibited similar functional aspects to primary human hepatocytes and may offer the opportunity to be used in energy metabolism studies (20). Therefore, it was hypothesized that *in vitro* models of NAFLD using HepaRG cells may be preferable for assessing mitochondrial respiratory changes.

The most important hallmark of NAFLD is lipid accumulation in the liver (21). Since oleic and palmitic acids are the most abundant FFAs in the serum of patients with NAFLD; they are commonly used to induce steatosis in *in vitro* models, usually at a ratio of 2/1 (13,22). Clinical studies have demonstrated that patients with NAFLD have an increased capacity to mobilize FFAs from adipose tissue to the liver, particularly when they suffer from insulin resistance (23,24). Despite the current debates about the sequence of events, it is well-documented that the chronic dysregulation of lipid homeostasis in hepatocytes leads to the increased production of toxic lipid intermediates, resulting in altered mitochondrial functions and lipotoxic effects (oxidative stress, insulin resistance, inflammation and hepatocyte injury) (25,26).

The present study aimed to assess cellular energy metabolism, particularly mitochondrial respiration and lipotoxicity in FFA-treated HepaRG and HepG2 cells. The findings presented herein may enable a more appropriate use of these 2D *in vitro* models regarding the changes in mitochondrial respiratory adaptations in the pathogenesis of NAFLD.

Materials and methods

Cells and cell culture. HepaRG cells (HRP101, liver cancer cells) were purchased from Biopredic International and cultured at a density of 26,600 cells/cm^2 as previously described (27). The cells were cultured in proliferation medium [William's E Medium (Lonza Group, Ltd.) supplemented with 5 μg/ml insulin, 50 μM hydrocortisone, 1% L-glutamine, 1% mixture of penicillin (10,000 UI/ml), streptomycin (10 mg/ml) and 10% fetal bovine serum] for 14 days. After that, the cells were cultured in proliferation medium supplemented with 1.5% dimethyl sulfoxide for a further 14 days. The cells were incubated at 37˚C in a 5% CO_2, 95% air-humidified atmosphere, and the medium was changed three times a week. HepaRG cells were then trypsinized and seeded in various well plates according to recommended densities (Biopredic International) and allowed to attach for 24 h (in proliferation medium) before free fatty acid treatments were applied.

HepG2 cells (ECACC85011430, liver cancer cells) were purchased from ECACC, and cultured in Minimum Essential Medium (Merck Life Science UK, Ltd.) supplemented with 1% non-essential amino acids, 10% fetal bovine serum, a 1% mixture of penicillin (10,000 UI/ml) and streptomycin (10 mg/ml) and 1% sodium pyruvate. The cells were incubated at 37˚C in a 5% CO_2, 95% air-humidified atmosphere and passaged once a week at 75% confluency. HepG2 cells were also allowed to attach for 24 h prior to exposure to FFAs.

Preparation of FFA treatments. Sodium oleate (OA) and sodium palmitate (PA) were purchased from Merck & Co., Inc. As previously described (28), 40 mM stock solutions of OA and PA were first prepared in 0.1 M NaOH (Merck & Co., Inc.), followed by conjugation to bovine serum albumin (BSA) (Merck & Co., Inc.). OA was dissolved at 40˚C for 20 min and PA at 70˚C for 30 min; the stock solutions were stored at -80˚C for no more than 3 months. To prepare conjugations of FFAs and BSA, 40 mM stock solutions of OA and PA were dissolved and mixed with 20% BSA for 1 h to yield 8-mM stock solutions (pH 7.4). They were further dissolved in the culture medium (without fetal bovine serum) to yield the concentrations needed to treat cells. The 8-mM stock solutions were sterile-filtered prior to use. The molar ratio between FFAs and BSA was 5.3, and 2.5% BSA was used as the control. BSA is used in various studies as a control (15,28). Unless otherwise indicated, in all the methods described below, the cells were treated with 1 mM OA/PA (2/1) and 2 mM OA/PA (1/1) for 24 h.

Analysis of cellular metabolism in non-permeabilized cells. The extracellular flux analyzer Seahorse XFe-96 (Agilent Technologies, Inc.) was used to measure the cellular metabolism of non-permeabilized cells. Prior to the measurement, the culture media containing FFAs were replaced with assay medium [bicarbonate-free XF DMEM pH 7.4 (Agilent Technologies, Inc.) supplemented with 4 mM L-glutamine, 1 mM pyruvate and 1 g/l D-glucose] and the cells were incubated in a CO_2-free incubator for 1 h at 37˚C. The seeding density was 20,000 cells per well (HepaRG and HepG2 cells) and 10,000 per well (primary rat hepatocytes) (PRH) (Data S1). Two types of tests were used as follows:

i) Mito stress test: Following the measurement of basal respiration, a mitochondrial stress test was performed by sequential additions of 1 μM oligomycin, 1.2 μM carbonyl cyanide-4-(trifluoromethoxy)phenylhydrazone (FCCP), and 1 μM rotenone and antimycin A. Differences between oxygen consumption rate (OCR) values in response to respiratory modulators were used to calculate various mitochondrial parameters (basal, and maximum respiration, ATP-linked respiration, spare respiratory capacity, and proton leak respiration). The Mito stress test was performed in HepaRG, HepG2 cells and PRH.

ii) Glycolytic rate assay: To describe changes in glycolytic parameters, the basal acidification rate represented as the proton efflux rate was measured, and the maximal glycolysis was then induced by 1 μM rotenone and antimycin A followed by the addition of 20 mM 2-deoxyglucose as a glycolysis inhibitor. The glycolytic rate assay was performed only in HepaRG and HepG2 cells. All calculated parameters were normalized to the total protein concentration (BCA assay, Thermo Fisher Scientific, Inc.). Unless stated otherwise, the materials used in both tests were purchased from Merck & Co., Inc.

Analysis of mitochondrial respiration in permeabilized cells. As previously described (29), cell culture media with FFAs were replaced with mitochondrial assay solution (70 mM sucrose, 220 mM mannitol, 10 mM KH_2PO_4, 5 mM $MgCl_2$, 2 mM HEPES, 1 mM EGTA, 0.2% BSA and 4 mM ADP, pH adjusted with 10 M KOH to 7.4 at 37˚C) before measuring the respiratory activity in permeabilized cells using the Seahorse XFe96 analyzer. Cellular permeabilization was performed using the recombinant perfringolysin-O (XF-PMPR, Agilent Technologies, Inc.) at a final concentration of 1 nM prior to measurement (permeabilization allowed substrates to enter the cells). Complex I-driven respiration was stimulated by the addition of 10 mM pyruvate with 1 mM malate or 10 mM glutamate with 1 mM malate. Complex II-driven respiration was stimulated by adding 10 mM succinate with 10 μM rotenone. β-oxidation was stimulated by adding 40 μM palmitoyl-carnitine (PC) with 1 mM malate. After measuring the OCR in the basal state, 1.5 μM oligomycin was injected, followed by the addition of 4 μM FCCP and 1 μM antimycin A. Differences between OCR values in response to respiratory modulators were used to calculate various mitochondrial parameters [oxidative phosphorylation (OXPHOS, state 3), maximal respiratory capacity (MRC, state 3u) and LEAK (state 4o)] as previously described (30). The seeding density was 20,000 cells per well. Unless stated otherwise, the materials used here were purchased from Merck & Co., Inc.

Preparation of cellular homogenates. According to a previously described protocol (31), the cells were washed and harvested in phosphate-buffered saline using a cell scraper (Kisker Biotech GmbH & Co. KG). Following centrifugation (1,000 x g, 4˚C, 5 min) the phosphate-buffered saline was discarded, and the cell pellets were immediately frozen at -80˚C. The following day, on the day of the measurements, cell pellets were suspended in 20 mM hypotonic potassium phosphate buffer (pH 7.5), followed by four circles of freeze and thaw. The lysate was made homogenous by passing and expelling it several times through a 26 G syringe (B. Braun).

Measurement of mitochondrial respiratory enzyme activities. According to the previously described protocols (31,32), freshly homogenized cells were used to measure the activity of mitochondrial respiratory enzymes. Citrate synthase (CS) activity was measured in an assay mixture containing 100 mM potassium phosphate (pH 8), Triton X-100 0.1%, 0.1 mM 5,5'-dithiobis-(2-nitrobenzoic acid), 0.3 mM acetyl-CoA and 0.5 mM oxaloacetate. The activity was calculated from the linear increase in 5,5'-dithiobis-(2-nitrobenzoic acid) absorbance at 412 nm for 10 min. Complex I was measured in an assay mixture containing 25 mM potassium phosphate (pH 7.8), 3.5 g/l BSA, 80 μM 2,6-dichloroindophenol, 70 μM decyl-ubiquinone, 2 mM EDTA, 10 μM antimycin A and 0.2 mM nicotinamide adenine dinucleotide (NADH). 10 μM rotenone was used to inhibit the complex I. The activity of complex I was calculated from the linear decrease in 2,6-dichloroindophenol absorbance at 600 nm for 5 min. Complex II was measured in an assay mixture containing 80 mM potassium phosphate (pH 7.8), 1g/l BSA, 60 μM 2,6-dichloroindophenol, 50 μM decyl-ubiquinone, 2 mM EDTA, 10 μM antimycin A and 20 mM succinate. 0,5 mM thenoyltrifluoroacetone was used to inhibit the complex II. The activity of complex II was calculated from the linear decrease in 2,6-dichloroindophenol absorbance at 600 nm for 10 min. Complex III activity was measured in an assay mixture containing 25 mM potassium phosphate (pH 7.6), 50 μM decyl-ubiquinol, 2 mM EDTA, 4 mM sodium azide, 0.05% Tween-20, and 50 μM cytochrome c. 10 μM antimycin A was used to inhibit complex III. The activity of complex III was calculated from the linear increase of cytochrome c absorbance at 550 nm for 10 min. Decyl-ubiquinol was freshly prepared by dissolving decyl-ubiquinone in acidified ethanol at pH 4, then reduced by the addition of a few grains of sodium borohydride and vortexed till the solution became colorless. Complex IV activity was measured in an assay mixture containing 30 mM potassium phosphate (pH 7.4), and 50 μM freshly reduced cytochrome c. A total of 4 mM sodium azide was used to inhibit complex IV. The activity of complex IV was calculated from the decrease of cytochrome c absorbance at 550 nm for 10 min. Complex I-IV activities were normalized to CS activity. Unless stated otherwise, the materials used here were purchased from Merck & Co., Inc. All absorbances were quantified using Tecan Infinite M200 (Tecan Group, Ltd.).

Transmission electron microscopy (TEM). The cells were prepared for TEM as previously described (33). After washing the cells with 0.1 M cacodylate buffer (pH 7.2, Merck & Co., Inc.), the cells were fixed directly on the culture flask for 3 h at room temperature in 3% glutaraldehyde (diluted in 0.1 M cacodylate buffer, pH 7.2; Merck & Co., Inc.). Subsequently, the cells were washed in 0.1 M cacodylate buffer (pH 7.2) and post-fixed in 1% osmium tetroxide for 1 h at room temperature. After rinsing, the cells were dehydrated in graded alcohols (50, 75, 96 and 100%), then clarified in propylene oxide and embedded in a mixture of Epon 812 and Durcupan (polymerization for 3 days at 60˚C; Merck & Co., Inc.). Semi-thin sections were stained by 1% toluidine blue (for 3 min at 60˚C; Merck & Co., Inc.). Ultrathin sections were cut using Ultrotome Nova (LKB). The sections were collected onto formvar carbon-coated copper grids, counterstained with uranyl acetate and lead citrate, and then finally

examined under JEOL JEM-1400Plus TEM (120 kV; JEOL, Ltd.). Images were obtained with the integrated 8Mpix CCD camera and processed further using the software TEM Center (Ver. 1.7.3.1537, JEOL, Ltd.).

Lactate dehydrogenase (LDH) assay. To evaluate plasma membrane integrity, the LDH assay kit (Diagnostic Systems GmbH) was used to quantify LDH activity in cell culture medium and cell lysates according to the manufacturer's instructions. LDH leakage was then calculated from the LDH activities in the cell culture medium and the cell lysates.

Caspase assays. To detect the activity of the effector caspase-3 and the mitochondrial pathway initiator caspase-9, fluorescent probes purchased from Life Sciences, Inc. were used. The substrates for caspase-3 and -9 are Ac-DEVD-AMC (λex=360 nm, λem=465 nm) and Ac-LEHD-AMC (λex=350 nm, λem=450 nm), respectively. Activated caspase enzymes cleave these substrates to release fluorescent AMC, which is then detected using a fluorescent plate reader (Tecan Infinite M200; Tecan Group, Ltd.). The cells were lysed in lysis buffer (50 mM HEPES, 5 mM CHAPS and 5 mM DTT) and stored at -80˚C. The cell culture medium was also collected and stored at -80˚C. The samples containing the aforementioned substrates were quantified in assay buffer (20 mM HEPES, 0.1% CHAPS, 5 mM DTT and 2 mM EDTA). Data were normalized to the protein concentration (BCA reducing agent compatible assay, Thermo Fisher Scientific, Inc.). Unless stated otherwise, the materials used here were purchased from Merck & Co., Inc.

Measurement of reactive oxygen species (ROS) production. CM-H_2DCFDA (Invitrogen; Thermo Fisher Scientific, Inc.) was used to evaluate the increased production of ROS. Its acetate groups are cleaved by intracellular esterases followed by subsequent oxidation yielding a fluorescent adduct (λex=485 nm, and λem=535 nm) that is trapped inside the cells. In brief, the HepaRG and HepG2 cells were incubated at room temperature with the indicator for 30 min (10 and 40 μM, respectively). The cells were washed with phosphate-buffered saline, and fluorescence was quantified using a fluorescent plate reader (Tecan Infinite M200; Tecan Group, Ltd.). Data were normalized to the protein concentration (BCA assay, Thermo Fisher Scientific, Inc.).

Measurement of mitochondrial membrane potential (MMP). MMP was quantified using the JC-1 fluorescent probe (Invitrogen; Thermo Fisher Scientific, Inc.) as previously described (34). JC-1 is a membrane-permeable cationic dye that exhibits potential-dependent accumulation in the mitochondria. At a higher MMP, it forms red fluorescence (λex=485 nm, and λem=590 nm), and at a lower MMP, it exhibits green fluorescence (λex=485 nm, and λem=525 nm). Briefly, the cells were incubated at room temperature with 20 μM JC-1 probe for 30 min, and after rinsing with cell culture medium, MMP was quantified using a fluorescent plate reader (Tecan Infinite M200; Tecan Group, Ltd.). Data are expressed as the red/green fluorescence ratio.

Oil Red O staining and triacylglycerol (TAG) quantification. To visualize TAG accumulation, the cells were stained with Oil Red O (Merck & Co., Inc.). The FFA-treated cells were fixed with 4% paraformaldehyde for 15 min at room temperature. Following fixation, the cells were stained with 0.5% Oil Red O for 15 min at room temperature before being observed under a light microscope (magnification, x40). According to the manufacturer's instructions, the TAG content was quantified using a TAG assay kit (Cayman Chemical Company). In brief, the attached cells were harvested from the cell culture plates using cell scrappers (Kisker Biotech GmbH & Co. KG), and where appropriate, detached cells were collected (940 x g, 4˚C, 5 min) from the culture media. Subsequently, all collected cells were sonicated and stored at -80˚C until spectrophotometric analyses. Data were normalized to protein concentration (BCA assay, Thermo Fisher Scientific, Inc.) or cell number.

RNA isolation and reverse transcription-quantitative polymerase chain reaction (RT-qPCR). Total cellular RNA was extracted using TRIzol® reagent (Invitrogen; Thermo Fisher Scientific, Inc.) from the FFA-treated cells. RNA was reverse transcribed using a cDNA Reverse Transcription kit (Applied Biosystems; Thermo Fisher Scientific, Inc.). The gene expression levels of fatty acid translocase (CD36), diacylglycerol O-acyltransferase 2 (DGAT2), peroxisome proliferator-activated receptor gamma coactivator 1-alpha (PPARGC1A), carnitine palmitoyltransferase 1A (CPT1A), peroxisome proliferator-activated receptor alpha gene (PPARA), hydroxy acyl-CoA dehydrogenase trifunctional multienzyme complex subunit alpha (HADHA), fatty acid synthase (FASN) and acyl-CoA dehydrogenase (LCAD) were quantified using the TaqMan Gene Expression probes, Hs00354519_m1, Hs01045913_m1, Hs00173304_m1, Hs00912671_m1, Hs00947536_m1, Hs00426191_m1, Hs01005622_m1 and Hs00155630_m1, respectively. The exact primer and probe sequences for our TaqMan Assays are proprietary; thus, the primer/probe sequences cannot be shared. However, the manufacturer provides the 'Context Sequence', which shows the sequence information of the probe and the amplicon of a TaqMan Assay (Table SI). Gene expression was analyzed using the Quant Studio 6 real-time PCR system (all obtained from Applied Biosystems; Thermo Fisher Scientific, Inc.). Data were normalized to polyubiquitin C RNA expression. mRNA levels were calculated using the comparative Cq method (2-ΔΔCq method) (35).

Statistical analysis. All experiments consisted of a minimum of three independent replicates. Statistical analysis was performed using GraphPad Prism 9.2.0 (GraphPad Software Inc.). Data are expressed as the mean ± SD. Following normality tests, two-way ANOVA followed by Tukey's post hoc multiple comparison tests was used to assess significance among groups in different cell lines. One-way ANOVA followed by Dunnett's post hoc multiple comparison tests was used to determine significance among groups in each cell line. A P-value <0.05 was considered to indicate a statistically significant difference.

Results

FFAs stimulate mitochondrial respiration and glycolysis in HepaRG cells, but not in HepG2 cells. Given that compared to cell lines, primary hepatocytes are considered a 'gold standard'

for cellular metabolism studies (36), the present study began by comparing mitochondrial respiration between PRH, and HepaRG and HepG2 cell lines following exposure to FFAs (the isolation process of the PRH is explained in Data S1). Firstly, the preliminary data from mitochondrial respiratory parameters calculated from OCR demonstrated that the FFA-treated PRH had a significantly lower basal respiration, maximal respiration, spare respiratory activity, proton leak and ATP-linked respiration, all compared to the FFA-treated HepaRG cells (P<0.001) (Fig. S1). On the contrary, no significant differences were found in the calculated mitochondrial parameters between the FFA-treated PRH and HepG2 cells. The study by Geng *et al* (28) demonstrated that the PRH and HepG2 cells had corresponding responses, including similar mitochondrial respiration after exposure to palmitic acid. As both the PRH and HepG2 cells exhibited a similar response concerning mitochondrial respiratory parameters following exposure to FFAs, the present study focused on comparing the HepaRG and HepG2 cells, particularly since they are both human liver cancer cells.

Although it is essential to study TAG accumulation and lipotoxicity caused by OA, PA, or combinations, assessing cellular metabolism to develop representative 2D *in vitro* models of NAFLD is equally vital. The present study primarily focused on evaluating the OCR and extracellular acidification rate (ECAR) following the exposure of the HepaRG and HepG2 cells to 1 mM OA/PA (2/1) and 2 mM OA/PA (1/1). It was established that compared to the FFA-treated HepG2 cells, the FFA-treated HepaRG cells had a significantly increased basal respiration (P<0.01), maximal respiration (P<0.01), spare respiratory activity (P<0.01), proton leak (P<0.001) and ATP-linked respiration (P<0.001) (Fig. 1). Accordingly, compared to the control, the mitochondrial parameters stated above were all significantly increased in the FFA-treated HepaRG cells. By contrast, these mitochondrial parameters were significantly decreased in the FFA-treated HepG2 cells compared with the control (apart from the proton leak at 1 mM) (Fig. 1).

As glycolysis is also an essential pathway in cellular metabolism (37), the present study measured the basal acidification caused by glycolysis. It was found that glycolysis parameters calculated from ECAR demonstrated that compared to the FFA-treated HepG2 cells, the FFA-treated HepaRG cells had significantly increased basal and compensatory glycolysis (P<0.001; Fig. 2A-C). Subsequently, compared to the control, the aforementioned glycolysis parameters were significantly increased in the FFA-treated HepaRG cells (P<0.05). By contrast, these glycolysis parameters were significantly decreased in FFA-treated HepG2 cells compared with control (P<0.001). The data from OCR and ECAR in both cell lines are summarized in a bioenergetic map shown in Fig. 2D.

FFAs increase complex I and II-driven respiration, and β-oxidation in HepaRG cells, but not in HepG2 cells. Having established that FFA stimulates mitochondrial respiration in HepaRG cells, but not in HepG2 cells, the present study then investigated which pathway leading into the Q-junction may be responsible for causing these outcomes. Our previously published studies on mouse models of NASH revealed a decreased complex II-driven respiration (38,39). Therefore, the present study evaluated OXPHOS, MRC and LEAK respiration in the presence of complex I-driven respiration substrates [pyruvate/malate and glutamate/malate (Fig. S2), complex II-driven respiration substrate (succinate), and β-oxidation substrates (PC/malate)]. It was found that compared to the FFA-treated HepG2 cells, the FFA-treated HepaRG cells exhibited a significantly increased OXPHOS [apart from 1 mM OA/PA (2/1) β-oxidation] and MRC in the presence of complex I substrates and β-oxidation (Fig. 3). Accordingly, in comparison to the controls, the data revealed stimulated complex I, II and β-oxidation driven OXPHOS in the FFA-treated HepaRG cells (P<0.05; Fig. 3B). On the other hand, the findings confirmed significantly decreased complex I, II and β-oxidation-driven OXPHOS in the FFA-treated HepG2 cells, all compared to the respective controls. The data also revealed that complex I-driven respiration (Figs. 3 and S2) and β-oxidation caused the highest LEAK respiration [>1.8-fold in the HepaRG cells exposed to 1 mM OA/PA (2/1)]. However, complex II-driven respiration in the HepaRG cells exposed to 1 mM OA/PA (2/1) did not significantly increase LEAK respiration, as shown in Fig. 3D.

The activity of complexes I and II is increased in FFA-treated HepaRG cells, but not in FFA-treated HepG2 cells. As other downstream mitochondrial respiratory enzymes and the mitochondrial content may also influence complex I, II-driven respiration and β-oxidation (31,40), the present study measured the activity of complexes I, II, III, IV and CS enzymes. It was confirmed that compared to the HepG2 cells, the HepaRG cells exhibited a 20±4% (P<0.001) greater activity of CS [a marker of mitochondrial content (41)] (Fig. 4A). Following treatment of the HepaRG cells with FFAs, their CS activity significantly decreased by 15±5% compared to the controls. By contrast, compared to the controls, the FFA-treated HepG2 cells demonstrated a 17±5% increase in CS activity (P<0.05). Notably, the activity of complex I was ~7-fold higher in the control HepG2 cells than in the control HepaRG cells (Fig. 4B). A high complex I activity is necessary for the proliferation of some cancer cells (42). In the present study, overall, complex I and II activity in the FFA-treated HepaRG cells was significantly increased (P<0.05) [apart from complex I in 1 mM OA/PA (2/1)]. On the contrary, compared to the controls, complex I and II activities were significantly decreased in the FFA-treated HepG2 cells (P<0.05). There was no significant difference in complex III activity compared to the control groups of both cell lines. As shown in Fig. 4D, there was no significant difference in complex III activity between the control and FFA-treated HepaRG cells. By contrast, compared to the controls, complex III activity was significantly decreased in the FFA-treated HepG2 cells (P<0.05). Of note, complex IV activity in the HepaRG cells was ~2.3-fold higher compared to the HepG2 cells (Fig. 4E). Complex IV plays a key role in OXPHOS, and HepaRG cells depend more on OXPHOS than HepG2 cells (43). There was no significant difference in complex IV activity between the control and FFA-treated HepaRG cells. On the other hand, in the HepG2 cells, complex IV activity in 2 mM OA/PA (1/1) was significantly decreased compared to the controls (Fig. 4E).

Exposure to FFAs disrupts the mitochondrial morphology of both HepaRG and HepG2 cells. Given that exposure to

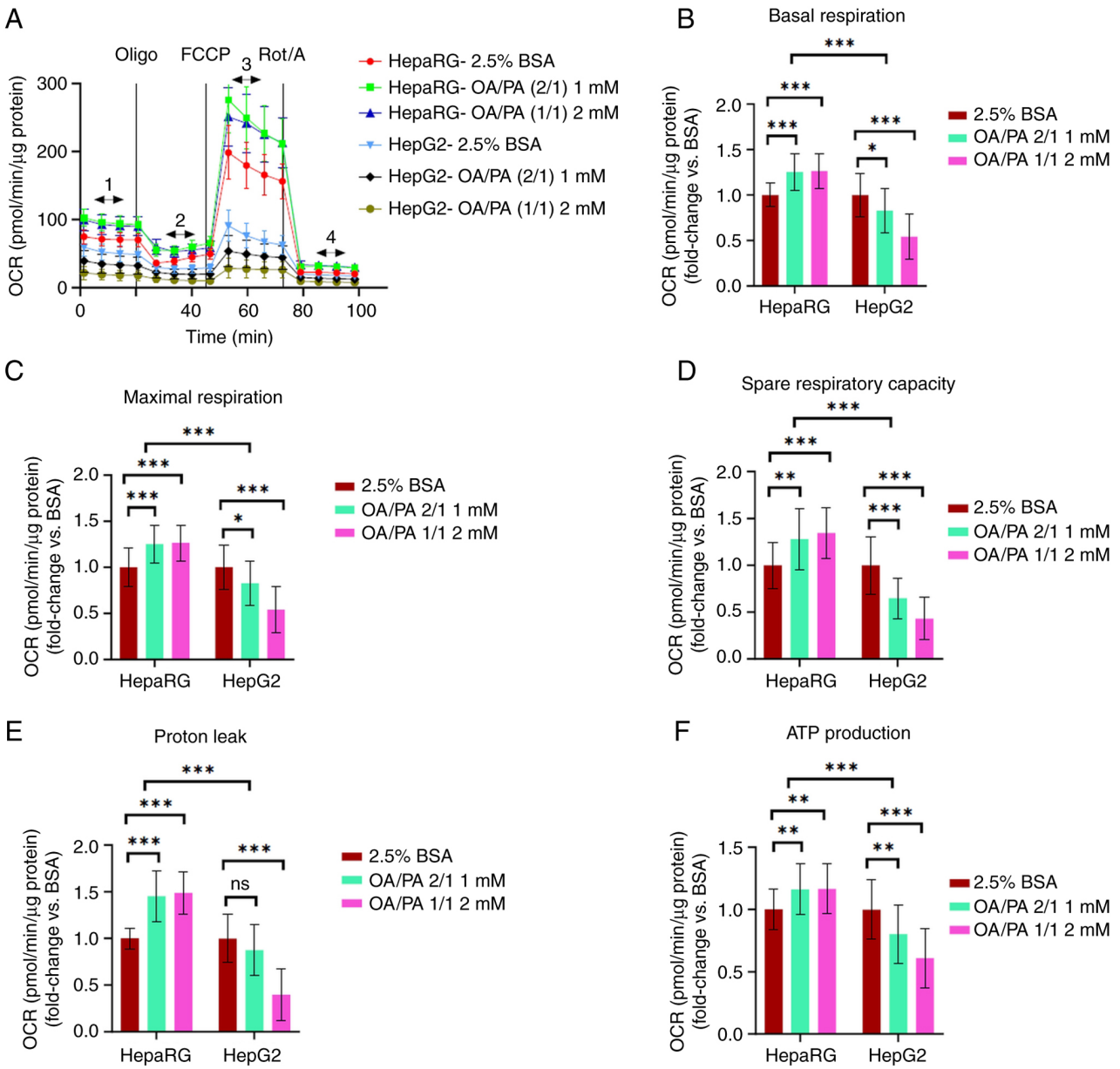

Figure 1. Calculated parameters of mitochondrial respiration in non-permeabilized HepaRG and HepG2 cells following exposure to free fatty acids. (A) Illustration of measurements that were performed, (B) basal respiration [1-4], (C) maximal respiration [3-4], (D) spare respiratory capacity [(3-1)-4], (E) proton leak [2-4], (F) ATP production-linked respiration [(1-2)-4]. Data are expressed as the mean ± SD. Statistical analyses were carried out using two- and one-way ANOVA followed by Tukey's and Dunnett's post hoc tests, respectively. *P<0.05, **P<0.01 and ***P<0.001. ns, not significant (n=32, B-F). OCR, oxygen consumption rate; OA, oleate; PA, palmitate; BSA, bovine serum albumin; Oligo, oligomycin; FCCP, carbonyl cyanide-p-trifluoromethoxyphenylhydrazone; Rot, rotenone; A, antimycin A.

FFAs may be associated with alterations in mitochondrial morphology (5), the present study used TEM to evaluate the number, size and ultrastructure of the mitochondria among all groups (control and FFA-treated cells). In addition, TEM was also used to evaluate the number and size of lipid droplets. It was found that the control HepG2 cells had fewer large mitochondria than the control HepaRG cells (Fig. 5). Exposure to FFAs altered the number, size and ultrastructure of the mitochondria in both HepaRG and HepG2 cells. Compared to the controls, HepaRG cells exposed to 1 mM OA/PA (2/1) exhibited smaller mitochondria with moderately disordered cristae. As shown in Fig. 5A, compared to the controls, HepaRG cells exposed to 2 mM OA/PA (1/1) also had smaller mitochondria, but with more disorganized cristae and dilutions of the matrix. Compared to the controls, the FFA-treated HepG2 cells exhibited numerous smaller mitochondria with disordered cristae and dilutions of the matrix, particularly following exposure to 2 mM OA/PA (1/1) (Fig 5B). In addition, it was confirmed that the quantity and size of lipid droplets increased with the concentrations of FFA in both cell lines (Fig. 5).

Lipotoxicity is induced to a greater extent in FFA-treated HepaRG cells than in FFA-treated HepG2 cells. As alterations in mitochondrial respiration and morphology are linked to lipotoxicity (5,44,45), the present study then evaluated the markers of cell death, mitochondrial damage and ROS production in

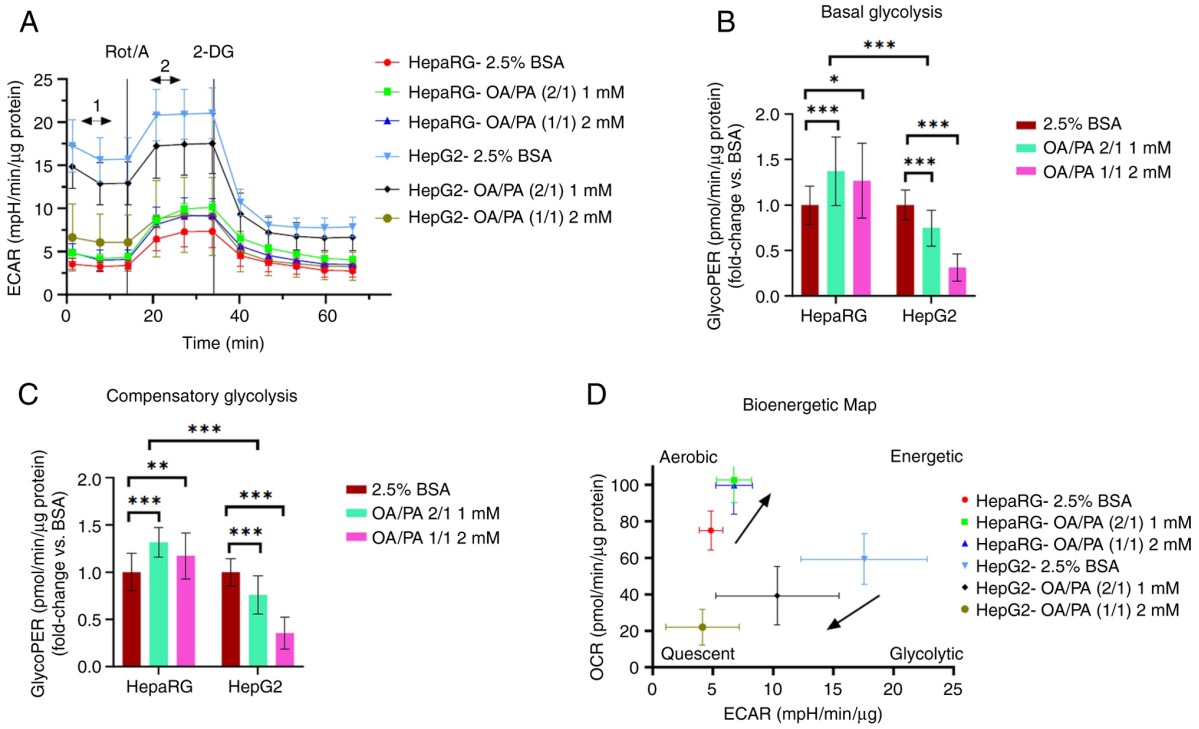

Figure 2. Calculated parameters of glycolysis and the bioenergetic map of HepaRG and HepG2 cells following exposure to free fatty acids. (A) Illustration of measurements that were performed, (B) basal glycolysis [1], (C) compensatory glycolysis [2], (D) bioenergetic map in the basal state. Data are expressed as the mean ± SD. Statistical analyses were carried out using two- and one-way ANOVA followed by Tukey's and Dunnett's post hoc tests, respectively. *P<0.05, **P<0.01 and ***P<0.001. (n=32, B-D). ECAR, extracellular cellular acidification rate, glycoPER, glycolysis proton efflux rate, OCR, oxygen consumption rate; OA, oleate; PA, palmitate; BSA, bovine serum albumin; 2 DG, 2-deoxy-d-glucose.

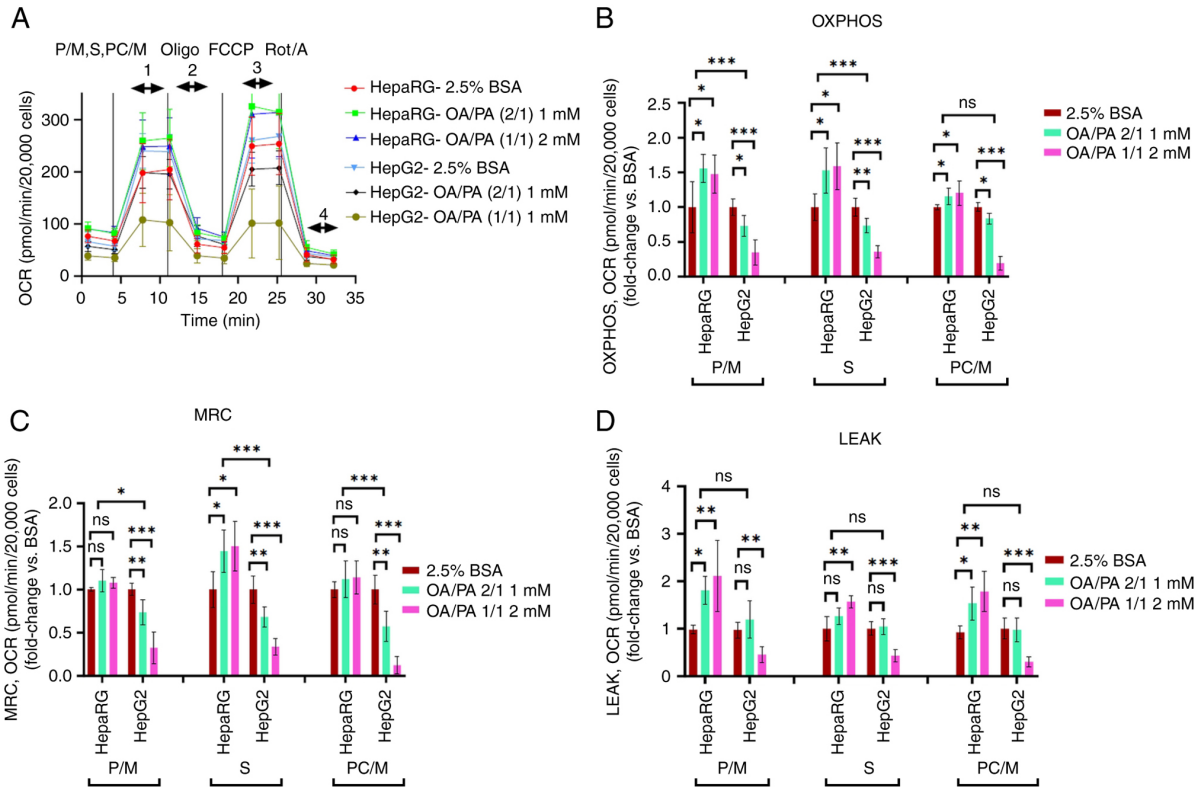

Figure 3. Calculated parameters of substrate-driven respiration in permeabilized HepaRG and HepG2 cells following exposure to free fatty acids. (A) Illustration of measurements that were performed. Added substrates were P/M, S and PC/M, (B) OXPHOS [state 3, (1-4)], (C) maximal respiratory capacity [MRC, state 3u, (3-4)], (D) LEAK respiration [state 4o, (2-4)]. Data are expressed as the mean ± SD. Statistical analyses were carried out using one- or two-way ANOVA followed by Dunnett and Tukey's post hoc tests, respectively. *P<0.05, **P<0.01 and ***P<0.001. ns, not significant (n=8). P/M, pyruvate/malate; S, succinate; PC/M, palmitoyl-carnitine/malate; OXPHOS, oxidative phosphorylation; OCR, oxygen consumption rate; Oligo, oligomycin; FCCP, carbonyl cyanide-p-trifluoromethoxyphenylhydrazone; Rot, rotenone; A, antimycin A.

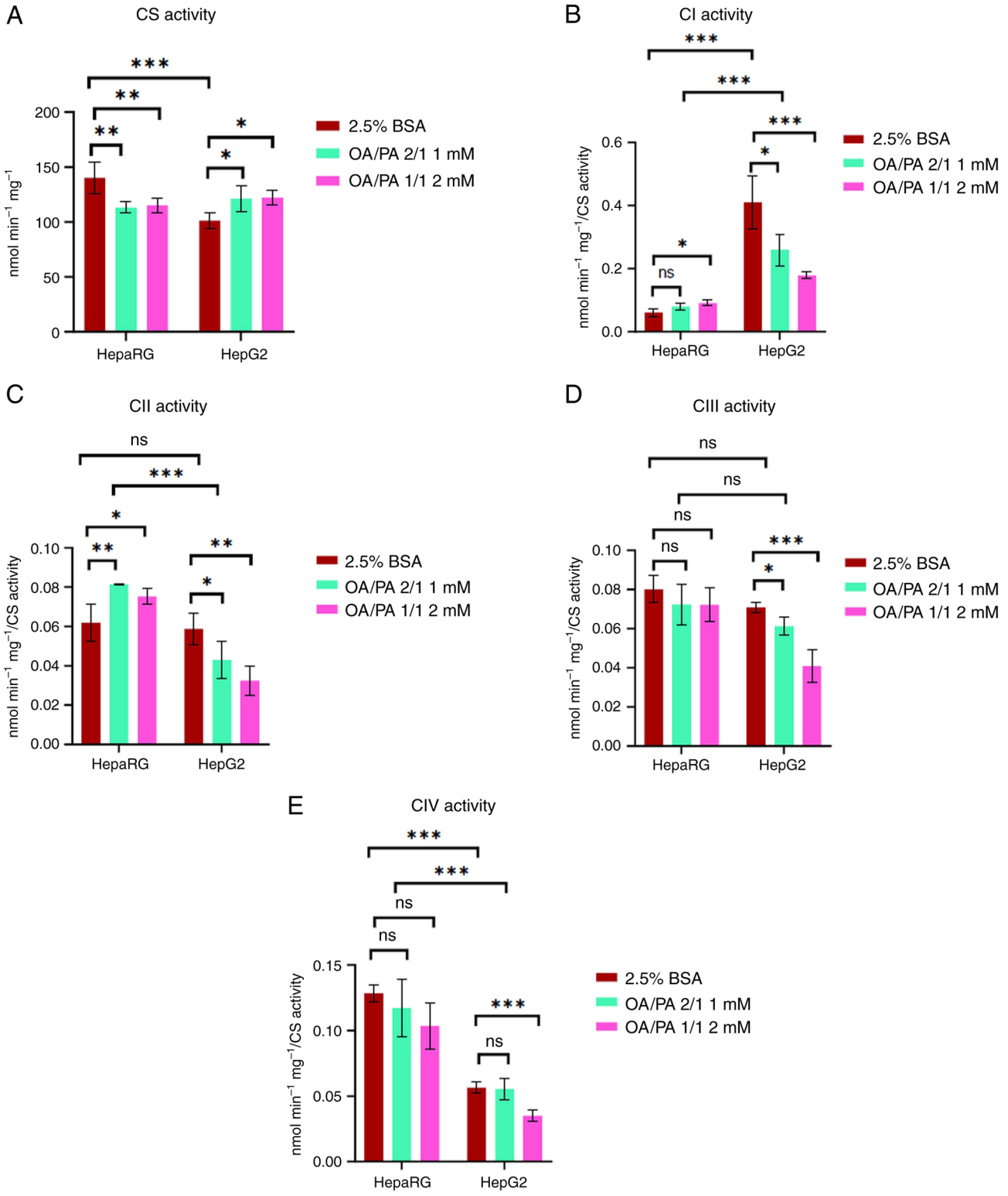

Figure 4. Activities of mitochondrial respiratory enzymes in HepaRG and HepG2 cells following exposure to free fatty acids. (A) CS activity, (B) CI activity, (C) CII activity, (D) CIII activity, (E) CIV activity. Data are expressed as the mean ± SD. Statistical analyses were carried out using two- and one-way ANOVA followed by Tukey's and Dunnett's post hoc tests, respectively. *P<0.05, **P<0.01 and ***P<0.001. ns, not significant; (n=4). CS, citrate synthase; CI, complex I; CII, complex II; CIII, complex III; CIV, complex IV; OA, oleate; PA, palmitate; BSA, bovine serum albumin.

both cell lines following exposure to FFAs. It was found that compared to the FFA-treated HepG2 cells, the FFA-treated HepaRG cells exhibited a significantly increased LDH leakage, caspase-3 activity and ROS production (P<0.001), as shown in Fig. 6A-D. In addition, the data presented in Fig. 6E revealed a decreased MMP in FFA-treated HepaRG cells compared to FFA-treated HepG2 cells (P<0.01). Subsequently, compared to the controls, a significantly increased LDH leakage, caspase-3 activity, caspase-9 activity and ROS production were observed in the FFA-treated HepaRG cells. Notably, no significant

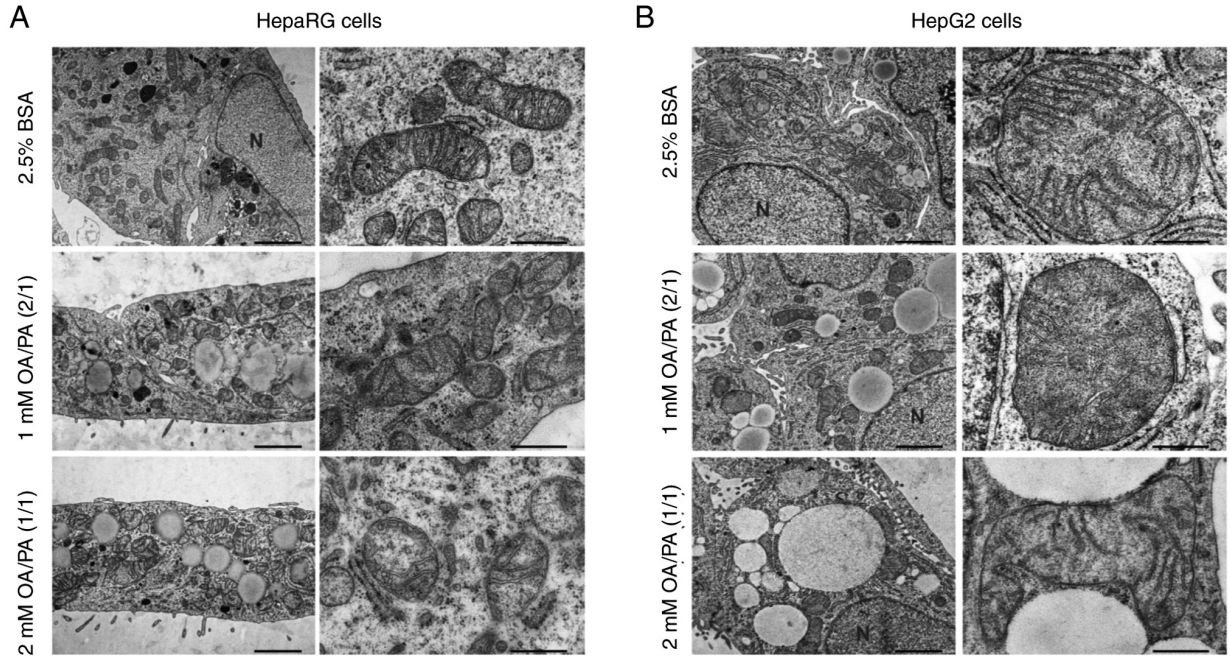

Figure 5. Transmission electron microscopy images of HepaRG and HepG2 cells following exposure to free fatty acids. The control HepG2 cells had fewer large mitochondria than the control HepaRG cells. FFA exposure altered the number, size and ultrastructure of the mitochondria in both HepaRG and HepG2 cells. (A) Compared to the controls, HepaRG cells exposed to 1 mM OA/PA (2/1) had smaller mitochondria with moderately disordered cristae. Compared to the controls, the HepaRG cells exposed to 2 mM OA/PA (1/1) also had smaller mitochondria, but with more disorganized cristae and dilutions of the matrix. (B) Compared to the controls, FFA-treated HepG2 cells had numerous smaller mitochondria with disordered cristae and dilutions of the matrix, particularly following exposure to 2 mM OA/PA (1/1). In addition, it was confirmed that the quantity and size of lipid droplets increased with the concentrations of FFA in both cell lines. OA, oleate; PA, palmitate; BSA, bovine serum albumin; N, nucleus. The scale bar of all images on the left panel of (A and B) is 2 μm. The scale bar of all images on the right panel of (A and B) is 500 nm.

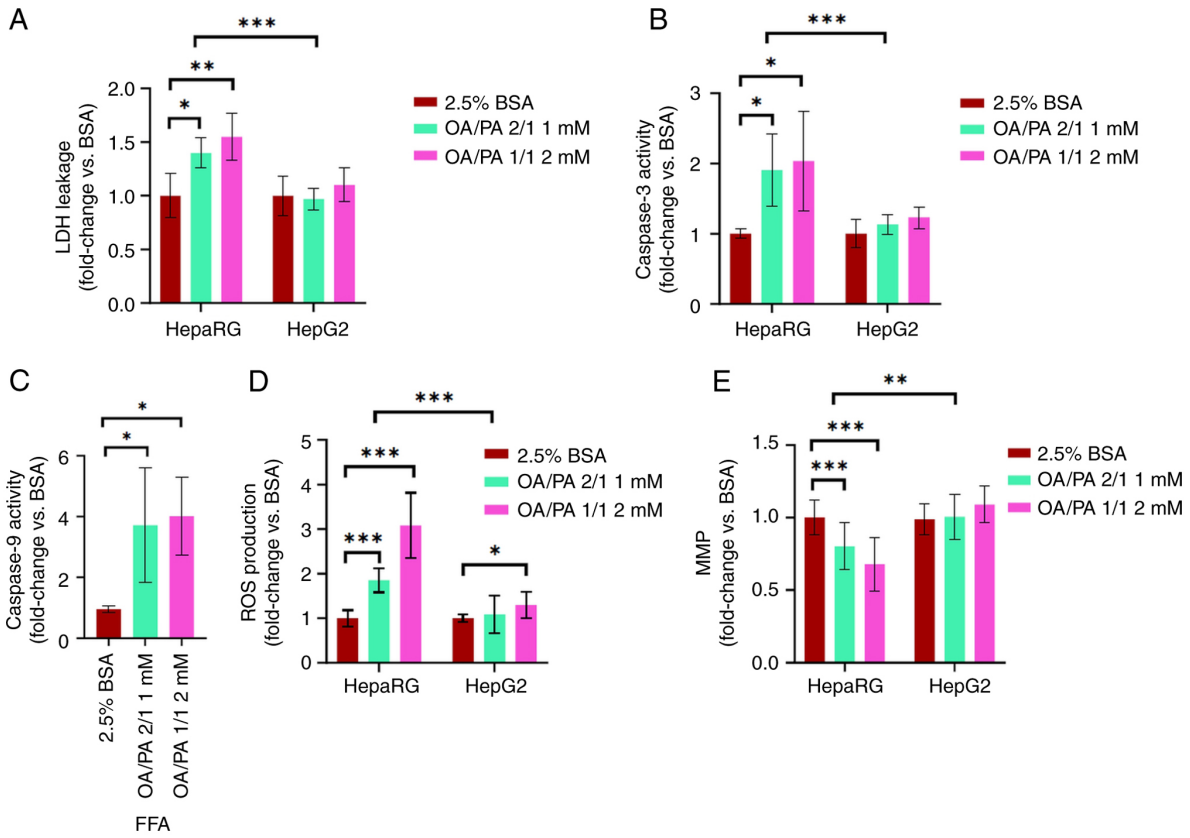

Figure 6. Lipotoxic effects of free fatty acids on HepaRG and HepG2 cells. (A) LDH leakage, (B) caspase-3 activity, (C) caspase-9 activity in HepaRG cells, (D) ROS production, (E) MMP. Data are expressed as the mean ± SD. Statistical analyses were carried out using two- and one-way ANOVA followed by Tukey's and Dunnett's post hoc tests, respectively. *P<0.05, **P<0.01 and ***P<0.001. (A-C) n=6 (D, E) n=16. LDH, lactate dehydrogenase; ROS, reactive oxygen species; MMP, mitochondrial membrane potential; OA, oleate; PA, palmitate; BSA, bovine serum albumin.

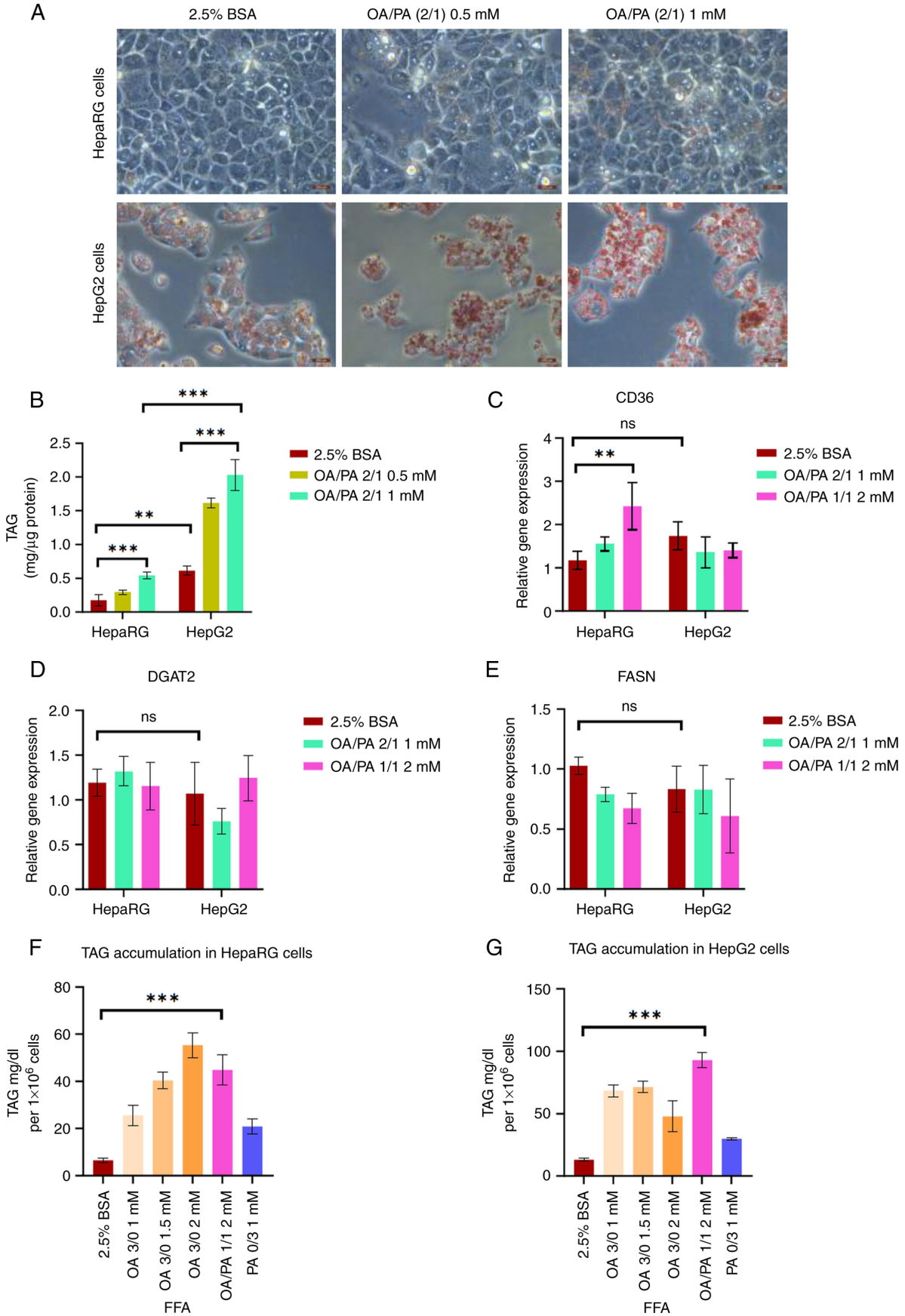

Figure 7. Effects of free fatty acids on TAG accumulation in HepaRG and HepG2 cells. (A) Lipid droplets were stained with Oil Red O and visualized under a light microscope (magnification, x40). (B) TAG content in both cell lines (n=6). Relative gene expression of (C) CD36, (D) DGAT2, and (E) FASN. (F) TAG content of various FFAs in HepaRG cells. (G) TAG content of various FFAs in HepG2 cells. Data are expressed as the mean ± SD. Statistical analyses were carried out using two- and one-way ANOVA followed by Tukey's and Dunnett's post hoc tests, respectively. **P<0.01 and ***P<0.001. ns, not significant. (C-E) n=6, (F, G) n=5. TAG, triacylglycerol; CD36, fatty acid translocase gene; DGAT2, diacylglycerol O-acyltransferase 2 gene; FASN, fatty acid synthase; OA, oleate; PA, palmitate; BSA, bovine serum albumin.

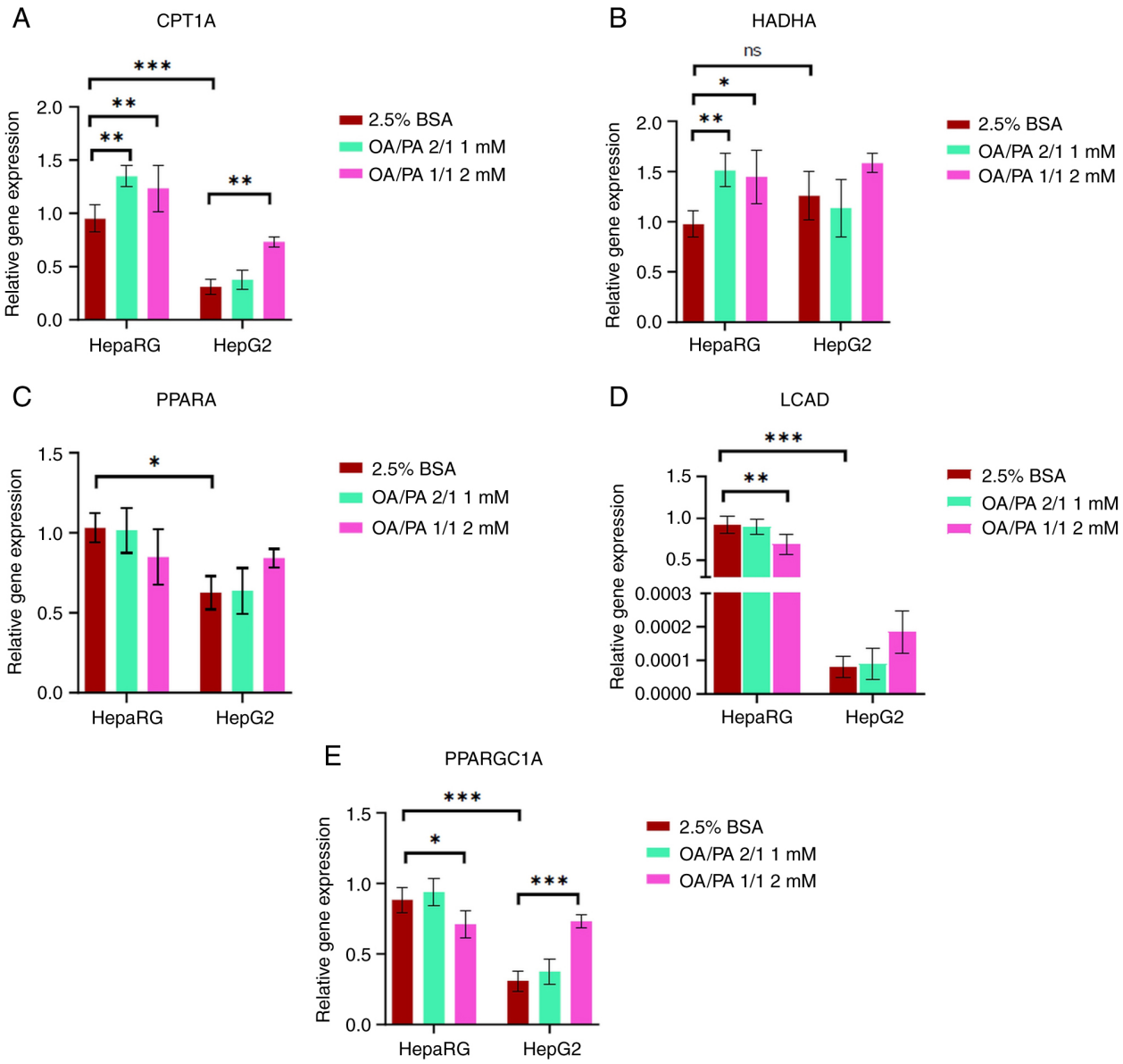

Figure 8. Relative expression of β-oxidation and mitochondrial biogenesis genes in HepaRG and HepG2 cells following exposure to free fatty acids. (A) CPT1A, (B) HADHA, (C) PPARA, (D) LCAD, and (E) PPARGC1A. Data are expressed as the mean ± SD. Statistical analyses were carried out using two- and one-way ANOVA followed by Tukey's and Dunnett's post hoc tests, respectively. *P<0.05, **P<0.01 and ***P<0.001. ns, not significant. (A-E) n=6. CPT1A, carnitine palmitoyltransferase 1A; HADHA, hydroxyacyl-CoA dehydrogenase trifunctional multienzyme complex subunit alpha; PPARA peroxisome proliferator-activated receptor alpha; LCAD, acyl-CoA dehydrogenase; PPARGC1A, peroxisome proliferator-activated receptor gamma coactivator 1-alpha; OA, oleate; PA, palmitate; BSA, bovine serum albumin.

differences were observed in LDH leakage, caspase-3 activity, MMP and ROS production (apart from ROS production at the 2 mM concentration) in the FFA-treated HepG2 cells. Caspase-9 activity in HepG2 cells is not shown as the level was below the detection limits.

HepaRG cells accumulate less TAG than HepG2 cells under the control and FFA-treated conditions. To confirm whether FFA exposure results in intracellular lipid accumulation, TAG accumulation was visualized and quantified in both cell lines following treatment with FFAs. It was confirmed that both cell lines accumulated intracellular lipids, even at a low concentration of 0.5 mM, as shown in Fig. 7A and B. However, the HepaRG cells accumulated significantly less TAG than the HepG2 cells. Following exposure to FFAs, the HepaRG cells accumulated 4-fold less TAG than the HepG2 cells. To assess whether the differences in TAG accumulation were caused by differences in FFA transport or TAG production, the mRNA expression of the fatty acid translocase (CD36) and the TAG synthesizing (FASN and DGAT2) genes was measured. It was confirmed that the mRNA expression of the fatty acid translocase (CD36), FASN and DGAT2 genes was similar in both cell lines (Fig. 7C-E). Subsequently, it was found that compared to other concentrations of FFAs, the concentration that caused the highest TAG accumulation without excessive cell death was 2 mM OA/PA (1/1) in both cell lines (Fig. 7F and G). Although 2 mM OA led to the highest TAG accumulation in the HepaRG cells (Fig. 7F), it was coupled with excessive cell death (data not shown).

Genes regulating β-oxidation and mitochondrial biogenesis are more highly expressed in HepaRG cells than in HepG2 cells. To further assess TAG accumulation and lipid metabolism in FFA-treated cells, the mRNA expression of genes regulating β-oxidation and mitochondrial biogenesis was measured. It was found that compared to the HepG2 cells, the HepaRG cells had a higher mRNA expression of β-oxidation-regulating genes [CPT1A ($P<0.001$), PPARA ($P<0.05$) and LCAD ($P<0.001$; ~10,000-fold)] and of the mitochondrial biogenesis-regulating gene (PPARGC1; $P<0.001$) (Fig. 8A and C-E). Moreover, compared to the controls, an increased mRNA expression of HADHA ($P<0.05$) (Fig. 8B) and a slightly increased expression of CPT1A (expression increased by <50%) were observed in the FFA-treated HepaRG cells. By contrast, the mRNA expression of HADHA and CPT1A in the FFA-treated HepG2 cells was the same as that in the controls (apart from the CPT1A gene at 2 mM).

Discussion

A greater variety and number of *in vitro* models suitable for studying mitochondrial respiratory adaptations following exposure to FFAs are required (13). The present study assessed cellular energy metabolism, particularly mitochondrial respiration and lipotoxicity in FFA-treated HepaRG and HepG2 cells. The findings revealed that compared to the HepG2 cells, the HepaRG cells were more suitable for studying mitochondrial respiratory adaptations in the developed early model of NASH.

Mitochondria are an essential target for lipid metabolism studies as they coordinate bioenergetic functions and maintain cellular homeostasis by responding to changes in the cellular environment, such as substrate flux and cellular stress (26). There are contradictory reports from *in vitro, in vivo* and clinical studies on mitochondrial respiration in NAFLD (8,11). However, various clinical studies have provided evidence of an augmented TCA flux, β-oxidation and mitochondrial respiratory chain activity in patients with simple steatosis or early-stage NASH (9,10). Although the majority of studies using HepG2 cells have revealed a decreased mitochondrial respiration following exposure to FFAs, the use of HepaRG cells has not yet been fully explored (13). To that end, the present study assessed and compared mitochondrial respiration, glycolysis, mitochondrial morphology, ROS production, MMP, TAG accumulation, and cell death markers in FFA-treated HepaRG and HepG2 cells. The present study revealed that FFA-treated HepaRG cells exhibited an increased mitochondrial respiration, glycolysis, mitochondrial fragmentation, ROS production, TAG accumulation, cell death and decreased MMP. The findings from the HepaRG cells are in accordance with the majority of studies supporting an increased mitochondrial respiration associated with a high ROS production in early-stage NASH (8-10,46). They are also consistent with the early-stage NASH model proposed by Feaver *et al* (47) which used a coculture of primary human hepatocytes and nonparenchymal cells to show that stimulated β-oxidation and ATP production occurred in parallel with lipotoxicity following exposure to FFAs. On the other hand, herein, the FFA-treated HepG2 cells exhibited a decreased mitochondrial respiration, increased ROS production [2 mM OA/PA (1/1)], mitochondrial fragmentation and TAG accumulation, with no change in MMP and cell death. The findings demonstrating a decreased mitochondrial respiration in FFA-treated HepG2 cells are in accordance with those of previous studies, although the findings regarding lipotoxicity are inconsistent (15,16,45,48).

The analyzed parameters in non-permeabilized cells revealed that mitochondria in the HepaRG cells adapted to increased lipid accumulation by stimulating basal and leak respiration, as an attempt to reduce accumulated fats by increasing their oxidation beyond the control of ATP synthase in coupled respiration. Pharmacological agents uncoupling the mitochondrial respiration of hepatocytes have been shown to reverse hepatic steatosis and insulin resistance in a rodent model of NAFLD (49). Moreover, increased maximal respiration, spare respiratory capacity and ATP-linked respiration reflect the ability of FFA-treated HepaRG cells to cope with exacerbated energy demands under acute cellular stress. At the same time, the FFA-treated HepG2 cells and PRH (Fig. S1) may not cope with the increased cellular energy demands due to a decreased ATP content, a feature observed in the late stages of NASH (50). Experiments using permeabilized cells corroborated the findings from non-permeabilized cells by showing increased complex I, and II-driven respiration in FFA-treated HepaRG cells. Although the activities of complexes III and IV did not differ significantly among the groups, increased complex I and II activity likely stimulated complex I and II-driven respiration in FFA-treated HepaRG cells. In addition, it was also affirmed that complex I-driven respiration and β-oxidation (PC/M) are likely responsible for increasing ROS production as they had the most LEAK-driven respiration compared to complex II-driven LEAK respiration. An increased leak respiration reflects an electron leak linked to ROS production (51). Although there are various ROS producers within the mitochondria, complex I, III and β-oxidation have been identified as some of the significant ROS production sites (52,53). The stimulated β-oxidation in the presence of PC/malate was also supported by increased expression of the genes controlling β-oxidation in FFA-treated HepaRG cells. Knockout studies have demonstrated that mice lacking the HADHA gene have a decreased β-oxidation (54). By contrast, HepG2 cells exposed to FFAs showed decreased complex I and II driven respiration, confirmed by decreased activities of complexes I, II, III and IV [apart from 1 mM OA/PA (2/1)]. The findings from HepG2 cells are in accordance with those of previous studies showing decreased complex I, II, III, and IV activities in FFA-treated HepG2 cells (16,45). In addition, analysis from ECAR confirmed that HepG2 cells have significantly higher glycolysis than HepaRG cells (55,56). Glycolysis was stimulated in FFA-treated HepaRG cells, but not in FFA-treated HepG2 cells. High glycolysis in cancer cells may also explain their increased complex I activity, which may be necessary to maintain a favorable NAD^+/NADH ratio to drive glycolysis and cell proliferation (42,57). Accordingly, the findings from HepaRG cells are in accordance with those from mice on a high-fat diet, demonstrating the concurrent stimulation of β-oxidation, glycolysis (58) and ROS production (59). All these findings suggest that FFA-treated HepaRG cells displayed the critical adaptive mechanism of 'mitochondrial flexibility'. By contrast, FFA-treated HepG2 cells failed

to show this vital mechanism under the current conditions. A progressive loss of 'mitochondrial flexibility' has been implicated in developing and progressing obesity-related comorbidities such as NAFLD (26).

Despite the attempts to decrease TAG accumulation by increasing mitochondrial respiration, in the long run, mitochondrial adaptations are insufficient to prevent lipotoxicity (5). This occurs as the adaptive responses also favor augmented ROS production. After all, more electrons enter the mitochondrial respiratory chain, likely increasing their chances of inappropriately reacting with molecular oxygen and causing mitochondrial and cellular damage (5). On that note, various attempts have been made to develop mitochondrial-targeted antioxidants, and some of these compounds have shown promising results in *in vitro* and *in vivo* NAFLD studies (60,61). An increased ROS production in FFA-treated HepaRG cells resulted in mitochondrial damage by increasing mitochondrial fragmentation, distorting cristae, decreasing mitochondrial content and inducing apoptosis. Although excessive mitochondrial fragmentation is detrimental, it is also associated with adaptive responses as it activates fatty acid β-oxidation and mitophagy (62). Exposure to FFAs has been shown to be associated with increased mitochondrial fission proteins and decreased fusion proteins in HepG2 cells (44,45,48). For HepaRG cells, 24-h exposure to FFAs was ideal as it allowed the authors to capture the coexistence of physiologically incompatible processes (in the long run), such as stimulated mitochondrial respiration and mitochondrial damage. After all, prolonged exposure to FFAs will eventually cause severe damage to the mitochondria and lead to a decline in mitochondrial respiration followed by cellular demise. On the other hand, it was surprising to observe that a significant decline in mitochondrial respiration in FFA-treated HepG2 cells did not result in more severe mitochondria damage and decreased cell viability. It is possible that the methods used to evaluate cell death in the present study may not have been as sensitive as those used in previous studies (45,48). Of note, the study by Doczi *et al* (63) demonstrated that the viability of HepG2 cells was not decreased by the complete inhibition of mitochondrial respiration. Nonetheless, in agreement with the study by Amorim *et al* (15), the FFA-treated HepG2 cells exhibited compensatory mitochondrial proliferation marked by the increased expression of the PPARGC1A gene and citrate synthase activity, secondary to excessive mitochondrial damage. The disruptions mentioned above are a mark of lipotoxicity, a complex process involving the deleterious effects of FFAs and FFA-intermediates, leading to oxidative stress, inflammation, insulin resistance, and cell death (NAFLD progression) (64).

Hepatic lipid accumulation is the hallmark of NAFLD (21), and the present study confirmed an associated increase in TAG accumulation with the increased concentrations of FFAs in both cell lines. However, the HepaRG cells had a 4-fold lower TAG content than the HepG2 cells. The expression of FFA transporter and TAG synthesis genes was similar in both cell lines; therefore, it could not provide a plausible reason. On the other hand, compared to the HepG2 cells, the HepaRG cells had a higher expression of β-oxidation regulating genes and mitochondrial content. As previously demonstrated, LCAD gene knockout mice develop hepatic steatosis due to decreased β-oxidation (65). Based on the current data, it was speculated that compared to the HepG2 cells, the HepaRG cells could decrease their relatively low TAG content by increasing β-oxidation, particularly since they have more mitochondria than HepG2 cells. Finally, the difference in the TAG content may also be explained by the difference in energy substrate preference. As the HepG2 cells are more glycolytic (55,56), they may preferably use glucose as the energy substrate over fatty acids. Although the present study provided possible speculations on the differences in TAG between these cell lines, it is worth noting that there are other plausible reasons described in the literature that may also contribute to this finding, namely the decreased secretion of low-density lipoproteins, low TAG hydrolyzing enzymes and genetic mutations (PNPLA3|148 M) observed in HepG2 cells (13).

Although the HepaRG cells provided similar findings to clinical studies of early NASH, it is also equally essential to highlight that 2D culture models are limited to optimally represent the microenvironment of hepatocytes *in vivo* (13). Therefore, this model could be further improved using cocultures or 3D cultures to improve its reliability.

In conclusion, the present study demonstrated that the HepaRG and HepG2 cells adapted differently to exposure to FFAs. It was revealed that stimulated mitochondrial respiration was associated with lipotoxicity in FFA-treated HepaRG cells, but not in FFA-treated HepG2 cells. These findings suggest that the HepaRG cells are more suitable for assessing mitochondrial respiratory adaptations in the developed *in vitro* model of early-stage NASH.

Acknowledgements

Not applicable.

Funding

The present study was supported by the Grant Agency of the Charles University (GA UK no. 336221 and SVV-2023-260656) and the INOMED project CZ.02.1.01/0.0/0.0/18_069/0010046, funded by the Ministry of Education, Youth and Sports of the Czech Republic and by the European Union.

Availability of data and materials

The datasets used and/or analyzed during the current study are available from the corresponding author on reasonable request.

Authors' contributions

TEM, ME, PŽ, ZČ and OK were involved in the conception and design of the study. TEM, ME, EP, PS, JM, JD, PŽ, DČ and AB were involved in data acquisition. TEM, HL and OK were involved in the writing of the original draft. TEM, ME, EP, HL, PS, JM, JD, PŽ, PP, ZČ and OK were involved in review and editing the manuscript. TEM and OK were involved in funding acquisition. TEM, ME, EP, PS, JM, JD, PŽ, PP, DČ and AB were involved in the investigative aspects of the study. TEM, ME, EP, PS, JM, JD, PŽ, PP, DČ, AB, ZČ and OK were involved in the study methodology. TEM, PP, ZČ and OK were involved in project administration. PP, ZČ and OK supervised

the study. ME, EP, HL, JD, PŽ, PP and OK were involved in data validation. TEM, PS and OK confirm the authenticity of all the raw data. All authors have read and approved the final version of the manuscript.

Ethics approval and consent to participate

The isolation of primary rat hepatocytes was approved by the Animal-welfare Body of the Charles University (Hradec Kralove, Czech Republic) and the Ministry of Education, Youth and Sports (approval no. MSMT-11265/2022-3).

Patient consent for publication

Not applicable.

Competing interests

The authors declare that they have no competing interests.

References

1. Younossi ZM, Koenig AB, Abdelatif D, Fazel Y, Henry L and Wymer M: Global epidemiology of nonalcoholic fatty liver disease-meta-analytic assessment of prevalence, incidence, and outcomes. Hepatology 64: 73-84, 2016.
2. Anderson EL, Howe LD, Jones HE, Higgins JPT, Lawlor DA and Fraser A: The prevalence of non-alcoholic fatty liver disease in children and adolescents: A systematic review and meta-analysis. PLoS One 10: e0140908, 2015.
3. Maurice J and Manousou P: Non-alcoholic fatty liver disease. Clin Med (Lond) 18: 245-250, 2018.
4. Chitturi S, Abeygunasekera S, Farrell GC, Holmes-Walker J, Hui JM, Fung C, Karim R, Lin R, Samarasinghe D, Liddle C, *et al*: NASH and insulin resistance: Insulin hypersecretion and specific association with the insulin resistance syndrome. Hepatology 35: 373-379, 2002.
5. Simões ICM, Fontes A, Pinton P, Zischka H and Wieckowski MR: Mitochondria in non-alcoholic fatty liver disease. Int J Biochem Cell Biol 95: 93-99, 2018.
6. Nassir F and Ibdah JA: Role of mitochondria in nonalcoholic fatty liver disease. Int J Mol Sci 15: 8713-8742, 2014.
7. Lu Q, Tian X, Wu H, Huang J, Li M, Mei Z, Zhou L, Xie H and Zheng S: Metabolic changes of hepatocytes in NAFLD. Front Physiol 12: 710420, 2021.
8. Sunny NE, Bril F and Cusi K: Mitochondrial adaptation in nonalcoholic fatty liver disease: Novel mechanisms and treatment strategies. Trends Endocrinol Metabolism 28: 250-260, 2017.
9. Koliaki C, Szendroedi J, Kaul K, Jelenik T, Nowotny P, Jankowiak F, Herder C, Carstensen M, Krausch M, Knoefel WT, *et al*: Adaptation of hepatic mitochondrial function in humans with non-alcoholic fatty liver is lost in steatohepatitis. Cell Metab 21: 739-746, 2015.
10. Satapati S, Sunny NE, Kucejova B, Fu X, He TT, Méndez-Lucas A, Shelton JM, Perales JC, Browning JD and Burgess SC: Elevated TCA cycle function in the pathology of diet-induced hepatic insulin resistance and fatty liver. J Lipid Res 53: 1080-1092, 2012.
11. Begriche K, Massart J, Robin MA, Bonnet F and Fromenty B: Mitochondrial adaptations and dysfunctions in nonalcoholic fatty liver disease. Hepatology 58: 1497-1507, 2013.
12. Green CJ, Parry SA, Gunn PJ, Ceresa CDL, Rosqvist F, Piche ME and Hodson L: Studying non-alcoholic fatty liver disease: The ins and outs of in vivo, ex vivo and in vitro human models. Horm Mol Biol Clin Investig 41: 10.1515/hmbci-2018-0038, 2018.
13. Ramos MJ, Bandiera L, Menolascina F and Fallowfield JA: In vitro models for non-alcoholic fatty liver disease: Emerging platforms and their applications. iScience 25: 103549, 2022.
14. Green CJ, Johnson D, Amin HD, Sivathondan P, Silva MA, Wang LM, Stevanato L, McNeil CA, Miljan EA, Sinden JD, *et al*: Characterization of lipid metabolism in a novel immortalized human hepatocyte cell line. Am J Physiol Endocrinol Metab 309: E511-E522, 2015.
15. Amorim R, Simões ICM, Veloso C, Carvalho A, Simões RF, Pereira FB, Thiel T, Normann A, Morais C, Jurado AS, *et al*: Exploratory data analysis of cell and mitochondrial high-fat, high-sugar toxicity on human HepG2 cells. Nutrients 13: 1723, 2021.
16. Garcia-Ruiz I, Solis-Munoz P, Fernandez-Moreira D, Munoz-Yague T and Solis-Herruzo JA: In vitro treatment of HepG2 cells with saturated fatty acids reproduces mitochondrial dysfunction found in nonalcoholic steatohepatitis. Dis Model Mech 8: 183-191, 2015.
17. Pérez-Carreras M, Del Hoyo P, Martín MA, Rubio JC, Martín A, Castellano G, Colina F, Arenas J and Solis-Herruzo JA: Defective hepatic mitochondrial respiratory chain in patients with nonalcoholic steatohepatitis. Hepatology 38: 999-1007, 2003.
18. Donato MT, Tolosa L and Gómez-Lechón MJ: Culture and functional characterization of human hepatoma HepG2 cells. Methods Mol Biol 1250: 77-93, 2015.
19. Gibbons GF, Khurana R, Odwell A and Seelaender MC Lipid balance in HepG2 cells: Active synthesis and impaired mobilization. J Lipid Res 35: 1801-1808, 1994.
20. Tascher G, Burban A, Camus S, Plumel M, Chanon S, Le Guevel R, Shevchenko V, Van Dorsselaer A, Lefai E, Guguen-Guillouzo C and Bertile F: In-depth proteome analysis highlights HepaRG cells as a versatile cell system surrogate for primary human hepatocytes. Cells 8: 192, 2019.
21. Berlanga A, Guiu-Jurado E, Porras JA and Auguet T: Molecular pathways in non-alcoholic fatty liver disease. Clin Exp Gastroenterol 7: 221-239, 2014.
22. Zhou Y, Orešič M, Leivonen M, Gopalacharyulu P, Hyysalo J, Arola J, Verrijken A, Francque S, Van Gaal L, Hyötyläinen T and Yki-Järvinen H: Noninvasive detection of nonalcoholic steatohepatitis using clinical markers and circulating levels of lipids and metabolites. Clin Gastroenterol Hepatol 14: 1463-1472.e6, 2016.
23. Donnelly KL, Smith CI, Schwarzenberg SJ, Jessurun J, Boldt MD and Parks EJ: Sources of fatty acids stored in liver and secreted via lipoproteins in patients with nonalcoholic fatty liver disease. J Clin Invest 115: 1343-1351, 2005.
24. Ipsen DH, Lykkesfeldt J and Tveden-Nyborg P: Molecular mechanisms of hepatic lipid accumulation in non-alcoholic fatty liver disease. Cell Mol Life Sci 75: 3313-3327, 2018.
25. Geng Y, Faber KN, de Meijer VE, Blokzijl H and Moshage H: How does hepatic lipid accumulation lead to lipotoxicity in non-alcoholic fatty liver disease? Hepatol Int 15: 21-35, 2021.
26. Tsilingiris D, Tzeravini E, Koliaki C, Dalamaga M and Kokkinos A: The role of mitochondrial adaptation and metabolic flexibility in the pathophysiology of obesity and insulin resistance: An updated overview. Curr Obes Rep 10: 191-213, 2021.
27. Stefela A, Kaspar M, Drastik M, Holas O, Hroch M, Smutny T, Skoda J, Hutníková M, Pandey AV, Micuda S, *et al*: 3β-Isoobeticholic acid efficiently activates the farnesoid X receptor (FXR) due to its epimerization to 3α-epimer by hepatic metabolism. J Steroid Biochem Mol Biol 202: 105702, 2020.
28. Geng Y, Villanueva AH, Oun A, Buist-Homan M, Blokzijl H, Faber KN, Dolga A and Moshage H: Protective effect of metformin against palmitate-induced hepatic cell death. Biochim Biophys Acta 1866: 165621, 2020.
29. Elkalaf M, Vaněčková K, Staňková P, Červinková Z, Polák J and Kučera O: Measuring mitochondrial substrate flux in recombinant Perfringolysin O-Permeabilized cells. J Vis Exp 13: 10.3791/62902, 2021.
30. Iuso A, Repp B, Biagosch C, Terrile C and Prokisch H: Assessing mitochondrial bioenergetics in isolated mitochondria from various mouse tissues using seahorse XF96 analyzer. Methods Mol Biol 1567: 217-230, 2017.
31. Spinazzi M, Casarin A, Pertegato V, Salviati L and Angelini C: Assessment of mitochondrial respiratory chain enzymatic activities on tissues and cultured cells. Nat Protoc 7: 1235-1246, 2012.
32. Elkalaf M, Tůma P, Weiszenstein M, Polák J and Trnka J: Mitochondrial probe methyltriphenylphosphonium (TPMP) inhibits the krebs cycle Enzyme 2-Oxoglutarate Dehydrogenase. PLoS One 11: e0161413, 2016.
33. Cechakova L, Ondrej M, Pavlik V, Jost P, Cizkova D, Bezrouk A, Pejchal J, Amaravadi RK, Winkler JD and Tichy A: A potent autophagy inhibitor (Lys05) enhances the impact of ionizing radiation on human lung cancer cells H1299. Int J Mol Sci 20: 5881, 2019.
34. Kucera O, Endlicher R, Rousar T, Lotkova H, Garnol T, Drahota Z and Cervinková Z: The effect of tert-butyl hydroperoxide-induced oxidative stress on lean and steatotic rat hepatocytes in vitro. Oxid Med Cell Longev 2014: 752506, 2014.

35. Livak KJ and Schmittgen TD: Analysis of relative gene expression data using real-time quantitative PCR and the 2(-Delta Delta C(T)) method. Methods 25: 402-408, 2001.
36. Nagarajan SR, Paul-Heng M, Krycer JR, Fazakerley DJ, Sharland AF and Hoy AJ: Lipid and glucose metabolism in hepatocyte cell lines and primary mouse hepatocytes: A comprehensive resource for in vitro studies of hepatic metabolism. Am J Physiol Endocrinol Metab 316: E578-E589, 2019.
37. Judge A and Dodd MS: Metabolism. Essays Biochem 64: 607-647, 2020.
38. Staňková P, Kučera O, Peterová E, Lotková H, Maseko TE, Nožičková K and Červinková Z: Adaptation of mitochondrial substrate flux in a mouse model of nonalcoholic fatty liver disease. Int J Mol Sci 21: 1101, 2020.
39. Staňková P, Kučera O, Peterová E, Elkalaf M, Rychtrmoc D, Melek J, Podhola M, Zubáňová V and Červinková Z: Western diet decreases the liver mitochondrial oxidative flux of succinate: Insight from a Murine NAFLD model. Int J Mol Sci 22: 6908, 2021.
40. Pfleger J: Measurements of mitochondrial respiration in intact cells, permeabilized cells, and isolated tissue mitochondria using the seahorse XF analyzer. Methods Mol Biol 2497: 185-206, 2022.
41. Larsen S, Nielsen J, Hansen CN, Nielsen LB, Wibrand F, Stride N, Schroder HD, Boushel R, Helge JW, Dela F and Hey-Mogensen M: Biomarkers of mitochondrial content in skeletal muscle of healthy young human subjects. J Physiol 590: 3349-3360, 2012.
42. Urra FA, Muñoz F, Lovy A and Cárdenas C: The mitochondrial complex(I)ty of cancer. Front Oncol 7: 118, 2017.
43. Peyta L, Jarnouen K, Pinault M, Guimaraes C, Pais de Barros JP, Chevalier S, Dumas JF, Maillot F, Hatch GM, Loyer P and Servais S: Reduced cardiolipin content decreases respiratory chain capacities and increases ATP synthesis yield in the human HepaRG cells. Biochim Biophys Acta 1857: 443-453, 2016.
44. de Sousa IF, Migliaccio V, Lepretti M, Paolella G, Di Gregorio I, Caputo I, Ribeiro EB and Lionetti L: Dose- and time-dependent effects of oleate on mitochondrial Fusion/Fission proteins and cell viability in HepG2 cells: Comparison with palmitate effects. Int J Mol Sci 22: 9812, 2021.
45. Sasi US, Sindhu G and Raghu KG: Fructose-palmitate based high calorie induce steatosis in HepG2 cells via mitochondrial dysfunction: An in vitro approach. Toxicol In Vitro 68: 104952, 2020.
46. Grasselli E, Baldini F, Vecchione G, Oliveira PJ, Sardão VA, Voci A, Portincasa P and Vergani L: Excess fructose and fatty acids trigger a model of non-alcoholic fatty liver disease progression in vitro: Protective effect of the flavonoid silybin. Int J Mol Med 44: 705-712, 2019.
47. Feaver RE, Cole BK, Lawson MJ, Hoang SA, Marukian S, Blackman BR, Figler RA, Sanyal AJ, Wamhoff BR and Dash A: Development of an in vitro human liver system for interrogating nonalcoholic steatohepatitis. JCI Insight 1: e90954, 2016.
48. Longhitano L, Distefano A, Amorini AM, Orlando L, Giallongo S, Tibullo D, Lazzarino G, Nicolosi A, Alanazi AM, Saoca C, *et al*: (+)-lipoic acid reduces lipotoxicity and regulates mitochondrial homeostasis and energy balance in an in vitro model of liver steatosis. Int J Mol Sci 24: 14491, 2023.
49. Perry RJ, Kim T, Zhang XM, Lee HY, Pesta D, Popov VB, Zhang D, Rahimi Y, Jurczak MJ, Cline GW, *et al*: Reversal of hypertriglyceridemia, fatty liver disease, and insulin resistance by a liver-targeted mitochondrial uncoupler. Cell Metab 18: 740-748, 2013.
50. Serviddio G, Bellanti F, Tamborra R, Rollo T, Romano AD, Giudetti AM, Capitanio N, Petrella A, Vendemiale G and Altomare E: Alterations of hepatic ATP homeostasis and respiratory chain during development of non-alcoholic steatohepatitis in a rodent model. Eur J Clin Invest 38: 245-252, 2008.
51. Jastroch M, Divakaruni AS, Mookerjee S, Treberg JR and Brand MD: Mitochondrial proton and electron leaks. Essays Biochem 47: 53-67, 2010.
52. Zorov DB, Juhaszova M and Sollott SJ: Mitochondrial reactive oxygen species (ROS) and ROS-induced ROS release. Physiol Rev 94: 909-950, 2014.
53. Zhao RZ, Jiang S, Zhang L and Yu ZB: Mitochondrial electron transport chain, ROS generation and uncoupling (Review). Int J Mol Med 44: 3-15, 2019.
54. Nassir F, Arndt JJ, Johnson SA and Ibdah JA: Regulation of mitochondrial trifunctional protein modulates nonalcoholic fatty liver disease in mice. J Lipid Res 59: 967-973, 2018.
55. Kamalian L, Douglas O, Jolly CE, Snoeys J, Simic D, Monshouwer M, Williams DP, Park BK, and Chadwick AE: The utility of HepaRG cells for bioenergetic investigation and detection of drug-induced mitochondrial toxicity. Toxicol In Vitro 53: 136-147, 2018.
56. Porceddu M, Buron N, Rustin P, Fromenty B and Borgne-Sanchez A: In vitro assessment of mitochondrial toxicity to predict drug-induced liver injury. Methods Pharmacol Toxicol 21: 283-300, 2018.
57. Calabrese C, Iommarini L, Kurelac I, Calvaruso MA, Capristo M, Lollini PL, Nanni P, Bergamini C, Nicoletti G, Giovanni CD, *et al*: Respiratory complex I is essential to induce a Warburg profile in mitochondria-defective tumor cells. Cancer Metab 1: 11, 2013.
58. Ye JH, Chao J, Chang ML, Peng WH, Cheng HY, Liao JW and Pao LH: Pentoxifylline ameliorates non-alcoholic fatty liver disease in hyperglycaemic and dyslipidaemic mice by upregulating fatty acid β-oxidation. Sci Rep 6: 33102, 2016.
59. Liemburg-Apers DC, Willems PH, Koopman WJ and Grefte S: Interactions between mitochondrial reactive oxygen species and cellular glucose metabolism. Arch Toxicol 89: 1209-1226, 2015.
60. Zheng Y, Wang S, Wu J and Wang Y: Mitochondrial metabolic dysfunction and non-alcoholic fatty liver disease: New insights from pathogenic mechanisms to clinically targeted therapy. J Transl Med 21: 510, 2023.
61. Amorim R, Simões ICM, Teixeira J, Cagide F, Potes Y, Soares P, Carvalho A, Tavares LC, Benfeito S, Pereira SP, *et al*: Mitochondria-targeted anti-oxidant AntiOxCIN(4) improved liver steatosis in Western diet-fed mice by preventing lipid accumulation due to upregulation of fatty acid oxidation, quality control mechanism and antioxidant defense systems. Redox Biol 55: 102400, 2022.
62. Chen W, Zhao H and Li Y: Mitochondrial dynamics in health and disease: Mechanisms and potential targets. Signal Transduct Target Ther 8: 333, 2023.
63. Doczi J, Karnok N, Bui D, Azarov V, Pallag G, Nazarian S, Czumbel B, Seyfried TN and Chinopoulos C: Viability of HepG2 and MCF-7 cells is not correlated with mitochondrial bioenergetics. Sci Rep 13: 10822, 2023.
64. Engin AB: What is lipotoxicity? Adv Exp Med Biol 960: 197-220, 2017.
65. Zhang D, Liu ZX, Choi CS, Tian L, Kibbey R, Dong J, Cline GW, Wood PA and Shulman GI: Mitochondrial dysfunction due to long-chain Acyl-CoA dehydrogenase deficiency causes hepatic steatosis and hepatic insulin resistance. Proc Natl Acad Sci USA 104: 17075-17080, 2007.